International Journal of Metallurgical Engineering 2013, 2(1): 47-51
DOI: 10.5923/j.ijmee.20130201.07

Influence of Boron on the Hardenability of Unalloyed and Low Alloyed Steel

Anjana Deva*, Saikat K. De, Vinod Kumar, M. Deepa , B.K. Jha

R&D Centre for Iron and Steel, Steel Authority of India Limited, Ranchi-834002, India

Abstract Boron exerts a large influence on mechanical properties of steel through microstructural control. It increases the hardenability of steel by retarding the heterogeneous nucleation of ferrite at the austenite grain surfaces and the decomposition kinetics of austenite to ferrite transformation are governed by its location and chemical state. To understand the effect of boron (~ 25 ppm) on microstructural evolution and change in continuous cooling transformation (CCT) diagram , a systematic study has been carried out using Gleeble thermo-mechanical simulator in unalloyed (C: 0.05 wt%; Mn: 0.2 wt%) and low alloyed (C: 0.2 wt%; Mn: 1.2 wt%: Cr: 0.15 wt%) steels. CCT diagrams, plotted for the onset and end of pearlitic, bainitic and martensitic reactions, consisted essentially of two C-curves and a remarkable difference was observed on comparing the results for both steels. It is interesting to note that bainite and martensite are completely absent even at higher cooling rate of 70°C/sec in the unalloyed steel with boron addition. In contrast, the addition of boron was observed to promote significant bainite formation even at a slower cooling rate of only 20°C/sec in the low alloyed steel. These contradicting effects on hardenability can be explained by the effect of boron in shifting only the upper C curve to the right for reconstructive transformation.

Keywords Boron, Cooling Rate, CCT, Unalloyed, Low Alloyed, Hardenability

1. Introduction

The increase in grain boundary area per unit volume of austenite provides an increase in the number of potential nucleation sites for the subsequent austenite to ferrite transformation, which accelerates the transformation rate[1]. For the same cooling condition, a bigger austenite grain size results in decrease in the Ar3 temperature leading to decrease in the volume percentage of ferrite fraction, and the effect is manifested in terms of increased hardenability. It is well established that boron increases hardenability of steel by retarding the heterogeneous nucleation of ferrite at the austenite grain surfaces [2-4]. It is probable that this effect is due to the reduction in interfacial energy as boron segregates to the grain boundaries. This in turn makes grain boundary less effective as heterogeneous sites. However, boron effect is entirely different in low and high carbon steels, plain and alloyed steels, with low and high soaking temperatures, and more significantly with low and high cooling rates.

Addition of boron increases the hardenability of quenched and tempered steels. However, the extent of hardening depends on transformation characteristics of austenite to ferrite and the presence of other alloying elements. A systematic study through thermo-mechanical simulator has been carried out in unalloyed and low alloyed steel to understand the boron effect on microstructural evolution and thereby change in continuous cooling transformation (CCT) diagram. Role of boron as a hardener under different soaking temperatures and cooling rates has also been examined.

* Corresponding author:
anjana@sail-rdcis.com (Anjana Deva)
Published online at http://journal.sapub.org/ijmee

2. Experimental

Chemical composition of aluminium killed boron added low C-Mn steel used in the present study is shown in Table 1.

Suitable test specimens were prepared from the crop ends of 32 mm transfer bar plates, collected after rough rolling of slabs. Specially designed tests were performed on the prepared specimens using Gleeble-3500C with fully integrated digital closed loop control thermal and mechanical system for understanding of processing conditions of hot rolling. Dilation tests aimed at determination of phase transformation temperatures. Easy to use Windows based computer software, combined with an array of powerful processors, provided an extremely user-friendly interface to create, run and analyze data from thermal-mechanical tests and physical simulation programs. Standards metallographic procedures were followed for material characterization which included optical microscopy. Scanning / transmission electron microscopy was used for characterizing low temperature phases and precipitates.

Table 1. Chemistry (wt. %) of unalloyed and low alloyed steels

Steel	C	Mn	P	S	Si	Al	Ti	Cr	B
Unalloyed	0.05	0.20	0.012	0.025	0.028	0.040	-	-	25 ppm
Low Alloyed	0.20	1.25	0.015	0.008	0.28	0.044	0.023	0.15	25 ppm

2.1. Dilatometric Study

The austenite to ferrite transformation is accompanied by increase in atomic volume of the transformed-phase; resulting dilation in the test specimen is linked with the kinetics of transformation[5,6]. A number of dilation plots were generated by exposing prepared tubular specimens (85 mm long with 10 mm diameter) of unalloyed steel at different austenitising temperatures followed by cooling them through varied rates as shown schematically in Fig.1. While austenitising, specimens were heated at the rate of 3°C/sec and soaked in the range of 950 to 1200°C for 120 seconds to facilitate homogenization of chemistry and microstructure. These specimens were then cooled at different rates, ranging from 1 to 70°C/sec. The change in diameter of these specimens during cooling was recorded using an ultra-sensitive dilatometer provided with the gleeble 3500 C simulator and the output of the dilatometer i.e. "dilatation plot" was used in identifying start and finish temperatures of transformed phase.

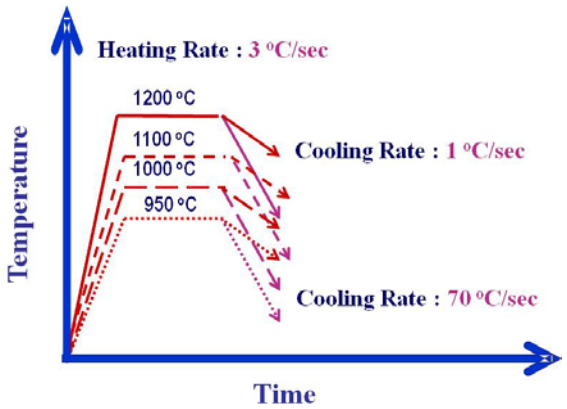

Figure 1. Schematic depiction of thermal cycles of dilatation study (unalloyed steel)

The steel samples of low alloyed steel were first soaked Ac3 temperatures (900°C) in the simulator for 120s, presuming that this will be adequate for chemical and structural homogenization. They were subsequently cooled to room temperature by employing cooling rates ranging from 0.2°C /sec to 36°C /sec.

3. Results and Discussion

Fig. 2 show a typical continuous cooling transformation (CCT) diagram of unalloyed boron added steel, constructed based on data generated on time taken for start to finish transformation for different cooling rates. It can be noted that with the increase in cooling rate, the onset of ferrite transformation shifted to a lower temperature.

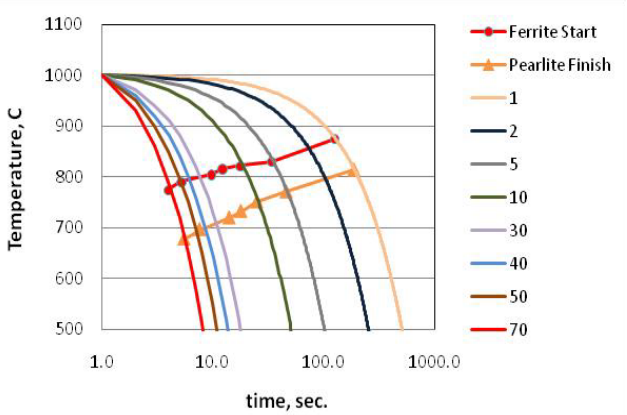

Figure 2. Continuous cooling transformation diagram of unalloyed steel

Sample heated to 1100°C and cooled with a rate of 70°C/sec was subjected to transmission electron microscopy. Figs. 3 (a-d) show the bright and dark field images alongwith selected area diffraction pattern and the indexed key. It may be noted that there is no evidence of martenisitic laths.

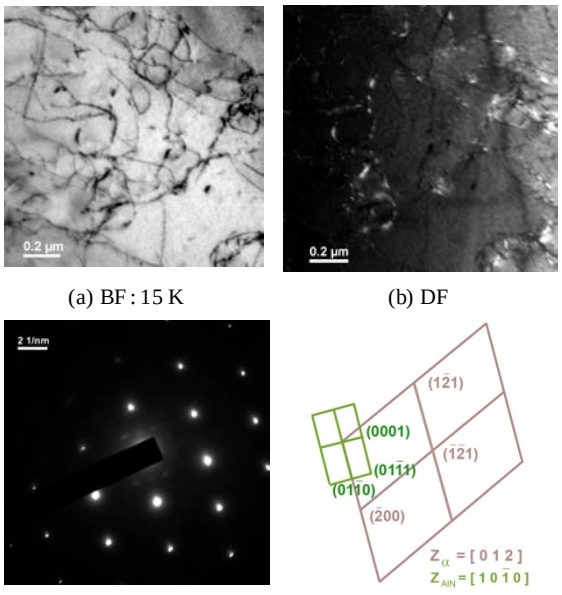

(a) BF : 15 K (b) DF

(c) SAD (d) Indexed key

Figure 3. Transmission Electron Micrographs depicting AlN precipitates

Dislocations entangled with the precipitates can be clearly seen here (Fig. 4a). From Fig. 4d, which shows the key of SAD, it is clear that the precipitates observed in dark field image shown in Fig. 4b are those of AlN with Z =[1 0 $\bar{1}$ 0].

Ferrite diffation pattern pertains to Z =[01 2].

To observe the microstructural evolution with much higher cooling rate, steel sample was heated to austenitisising temperature of 1200°C and subjected to very high cooling rate (~230°C/sec) in thermo-mechanical simulator and found that martensitic laths are present in steel (Fig. 4).

It clearly indicates that there must be a critical cooling rate, above which bainite or martensitic transformation starts in low carbon unalloyed steel also which will depend on soluble boron content, austenitising temperature and cooling rate.

It is interesting to note that the Ar3 temperatures of both the steels, when subjected to varied cooling rates, showed almost similar trend with the increase in cooling rate.

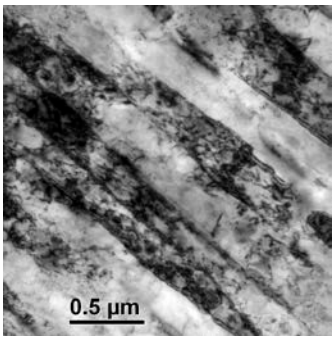

Figure 4. Bright field image (8K) showing martensitic laths at higher cooling rate

This observation authenticates that austenitisation at low temperature (950 °C) causes boron to precipitate as boron nitride leading to no dissolved boron in lattice. As a result, there is no contribution to hardenability of steel by boron and there is rather some amount of softening, owing to removal of free nitrogen through scavenging effect. Contrary to this phenomenon, a different kind of situation emergesd when boron treated steel was austenitised at higher temperatures (up to 1200 °C) followed by cooling at varied rates (Fig. 5).

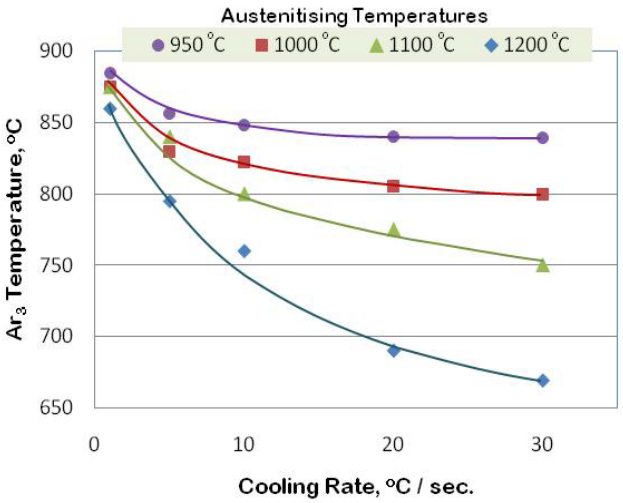

Figure 5. Variation in Ar3 temperature of B-added steel with cooling rate for different austenitising temperatures

The results show that increase in cooling rate leads to significant decrease in Ar3 temperature at higher austenitising temperatures (> 950°C). This effect is particularly greater at 1200°C.

Fig. 6 show a typical continuous cooling transformation (CCT) diagram of low alloyed boron added steel. Against each cooling rate curve Ar3, Ps, and Pf corresponding to proeutectoid ferrite start, pearlite start and pearlite finish temperatures respectively have been marked.

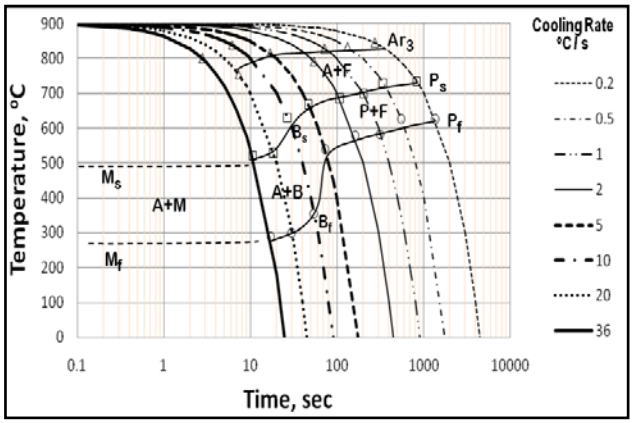

Figure 6. Continuous cooling transformation diagram of low alloyed steel

It can be inferred from Fig. 6 that at all the curves associated with different transformation temperatures have diminishing tendencies as the cooling rates are increased. However, decrease is gradual upto cooling rate of 5°C/s. The proclivity towards decline becomes quite sharp at and above cooling rates of 10°C/s, which continues till it again levels off at cooling rates of 20°C/s and beyond. The CCT diagram can be interpreted in terms of first formation of proeutectoid ferrite from austenite labeled Ar3 line in the figure. There is not much variations in this temperature with cooling rates. The region between Ar3 line and the Ps line gets widened upon increase in cooling rates. The lines representing Ps and Pf remain somewhat parallel upto cooling rate of 5oC/s. Marked change in width of separation occurs after this cooling rate and area get widened progressively as it approaches towards higher cooling rates. Therefore, cooling rate of 5oC/s is critical and seems to signal departure from formation of mere pearlite and ferrite phase mixture. This may also be the cooling rate above which bainite may form.

Fig. 7 show the scanning micrographs from samples cooled at different rates as indicated in the figure. The microstructures of Fig. 7 (a) and (b) from samples cooled at slower rates of 0.5°C/s and 2°C/s is completely dominated by ferrite and pearlite phase mixture.

However in the case of latter coarse peralite colony size is slightly bigger. The formation of proeutectoid ferrite has occurred along the prior austenite grain boundary. From this an estimate of average prior austenite grain size can be made, which works out to be ~130µm. The first indication of formation of bainite can be perceived in Fig. 7 (c). The bainite volume fraction has increased as can be discerned from Fig. 7 (d) obtained from sample cooled at the rate of

20°C/s. The above microscopic examinations corroborates the surmises gained from CCT diagram.

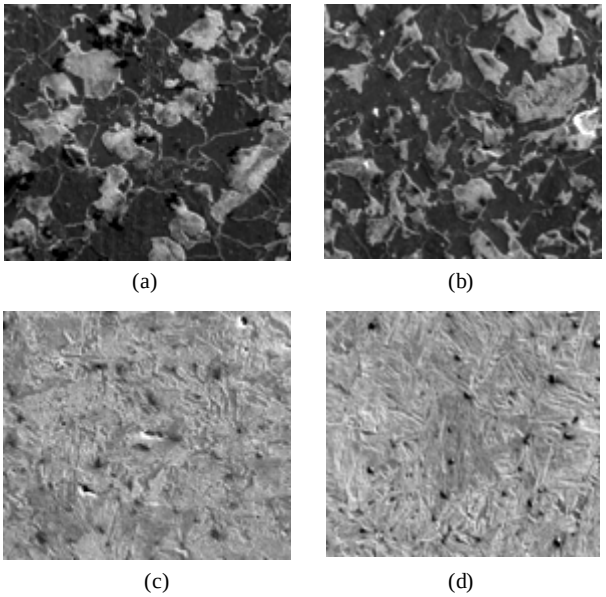

Figure 7. Scanning electron micrograph from samples (a) 0.2°C/s (b) 1°C/s (c) 10°C/s (d) 20°C/s

TTT diagrams are plotted for the onset and completion of reactions to form pearlite, bainite and martensite, consist essentially two C Curves, the one at higher temperature representing reconstructive transformation to ferrite or pearlite, and that at lower temperature where atomic mobility is diminished, representing displacive transformation such as Widmanstatten ferrite, bainite and acicular ferrite (Fig. 8).

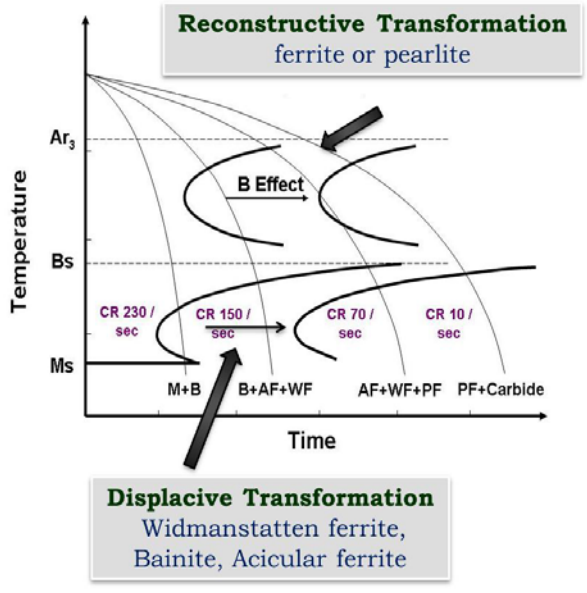

Figure 8. Schematic representation of boron on pronounced effect of upper C curve

Boron has the largest effect on the C-curve for reconstructive transformation, leaving the lower C-curve hardly changed. In Fig. 5, the effect of cooling rate on the evolution of microstructure has been shown schematically which further collaborates the pronounced effect of boron on upper C curve only.

The increase in incubation period before reconstructive transformation, as a function of soluble boron concentration has been investigated quantitatively by Pickering[7], and it was found, that there is proportional increase in the incubation period until a concentration of about 20 ppm is reached, after which the function becomes insensitive to boron and overall effect becomes unreliable. In contrast, for medium carbon (0.4 wt.%) high manganese (1.5 wt.%) steel, addition of boron (40 ppm) was observed to enable some bainite and martensite formation at a cooling rate of only 0.6 °C/sec[8]. Even slow cooling rate, as low as < 1 °C/sec has suppressed the formation of pearlite. In this case, the dramatic effect on hardenability can be attributed to shifting upper C curve to right by boron and shifting both upper and lower C curves to right by C and Mn.

4. Conclusions

• Both austenitising temperature and cooling rate are critical in influencing the hardenability of boron added steel.

• In unalloyed boron containing steel, no bainite/ martensite was formed even at cooling rate of 70°C/sec, whereas formation of theses phases occurred at much lower cooling rate of 20°C/sec in low alloyed boron added steel.

• It is not boron alone but its synergistic effect in presence of carbon, manganese, chromium has resulted in significant change in hardening behaviour of steel.

ACKNOWLEDGEMENTS

The authors thankfully acknowledge the guidance and support extended by the management of Research & Development Centre for Iron and Steel during the course of this work. Contribution by Ms Smriti Ojha, National Institute of Foundry and Forge Technology, Hatia, Ranchi during carrying out experiment is also acknowledged with thanks.

REFERENCES

[1] Ohmori Y. and Yamanaka K., Conference proceeding on Boron in Steel, edited by Banerjee S. K. and Morral J. E., The Metallurgical Society of AIME, Warrendale, PA, 1979, p.44.

[2] Shoenberger L. R., Trans AIME, 1958, Vol.212, p.402

[3] Cho Y.R. and Kim S.I., Iron and Steel Technology, May 2004, p.46.

[4] Tsuji, N., Matsubara, Y., Sakai, T., and Saito, Y., ISIJ International, Vol. 37, No 8, (1997), p.797.

[5] Grange R.A. and Mickel J.B.,Trans ASM, 1961, Vol. 53, p.157.

[6] Pandi, R., Militzer, M., Hawbolt, E.B. and Meadowcroft, T.R., 37th Mechanical Working and Steel Processing, ISS, (1996), p.635.

[7] Pickering F.B., Physical Metallurgy and the design of steel, Applied Science Publisher, London, 1978, p.50.

[8] Ohmori Y. and Yamanaka K., Conference proceeding on Boron in Steel, edited by Banerjee S. K. and Morral J. E., The Metallurgical Society of AIME, Warrendale, PA, 1979, p.44.